

Japan Geoscience Union Meeting 2011

(May 22-27 2011 at Makuhari, Chiba, Japan)

©2011. Japan Geoscience Union. All Rights Reserved.



MIS020-01

Room:301A

Time:May 24 14:15-14:30

Introduction

Yuki Kimura^{1*}

¹Tohoku University

We will introduce and discuss our purpose and future view in this session.

MIS020-02

Room:301A

Time:May 24 14:30-15:00

Nano-scale metrology for extra long-term prediction of global environmental change

Hisao Satoh^{1*}

¹Mitsubishi Materials Corporation

Global environmental change and energy problems are unavoidable issue for every human being. Although the utilization of nuclear power and fossil fuel are standing oppositely for emission of green-house gas, they are sharing common problem, wastes. Underground as the final destination of the wastes causes dissolution and precipitation of minerals toward the equilibrium. In the engineering fields for radioactive waste disposal and CCS (carbon capture and storage), long-term safety is predicted by computation based on limited kinetic data of interaction among groundwater, country-rocks, cement-buildings, and barrier-clay and on hydraulic behaviors.

In order to predict the underground condition for extra long-term period (~100 kyr), we need to obtain precise kinetic data in the order of $1E-5$ nm/s. During this period, rock and minerals should cause a few cm displacements, so that the groundwater flow can be changed. Latest metrological instruments (AFM and interferometer) are able to detect such an ultra-slow phenomenon. Interferometer is sometimes useful to reproduce the realistic reaction with in-situ measurement. I will here report the latest examples of (1) mineral dissolution measurements, (2) erosional dispersion of molecular layer by flow and (3) growth measurement of calcite, by using micro-interferometer with phase-shift optics.

Plagioclase, one of the most common rock-forming minerals, is poorly understood in its fundamental mechanisms of dissolution. In the most groundwater system, slightly alkaline pH promotes the dissolution. Dissolution process of Ca-bearing phases is important, because calcite and Ca-zeolite can be precipitated as the secondary phase. Dissolution experiments of anorthite (Satoh et al., 2007) and hornblende (Sato et al., in prep.) at alkaline conditions provided information about interface process accompanying with step retreat velocity, step density, and pH. Another experiment on dissolution measurement on zoned plagioclase suggested that solid-solution is controlling dissolution rates. Secondary phase precipitation was recognized in the process of high-pH dissolution of hornblende. Aggregates of colloidal precipitates deposited near etch pit and inhibited subsequent dissolution. Similar observation was made on olivine surface immersed in acidic solution. Amorphous Si-rich phase was recognized as secondary phase, which affects the dissolution process.

In natural system, clay can be eroded and dispersed into groundwater. Molecular layer can be lifted-up by swelling and DLVO repulsive force, and colloidized by flow. Interferometric measurement estimated possible colloid concentration (mol/m^3) of smectite, based on the observed colloidization rate ($\text{mol/m}^2/\text{s}$) and flow (m/s). Under a few hundred $\mu\text{m/s}$ of groundwater flow, ~10 ppb of colloid can be expected.

Growth rate of calcite is the most important information for CCS engineering. In the georeactor process by CO_2 -injection into hot-dry rock, carbon is fixed as calcite (Ueda et al., 2009). The growth rate of calcite is key information to evaluate the life-time of storage and the capacity. Laboratory in-situ measurement of calcite growth using high-T and high-P cell, and on-site experiment using Crystal Growth Sonde (Satoh, 2011) which enables deep-diving and in-situ growth were conducted to examine the system. The results showed that calcite growth is inhibited in the actual georeactor system in spite of sufficient supersaturation.

Thus, the mineral dissolution and growth in natural system tend to show slower rates. As a possible reason, widely existing and important, but forgotten impurity, colloid needs to be considered.

References

- [1] Satoh et al. (2007) *Am. Min.*, 92, 503-509.
- [2] Satoh et al. (in prep.)
- [3] King et al. (2010) *IMA 2010*, Abstract, 840.
- [4] Kurosawa et al. (2006) *Trans. Atom. Ener. Soc. Japan*, 5, 251-256.
- [5] Ueda et al. (2009) *Japanese Mag. Min. Petrol. Sci.*, 38, 220-231.
- [6] Satoh (2011) *The Review of High P. Sci. & Tech.*, 21 (in press).

Keywords: Nano-scale metrology, dissolution rate, growth rate, colloid, CO_2

MIS020-03

Room:301A

Time:May 24 15:00-15:30

Atomic-scale investigations of solid-liquid interfaces by frequency modulation atomic force microscopy

Hirofumi Yamada^{1*}

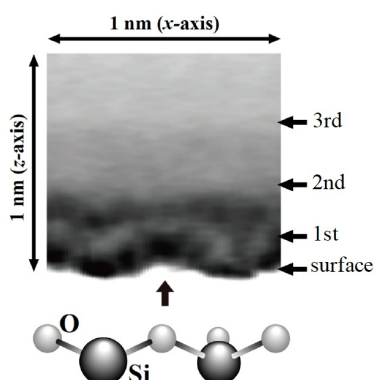
¹Grad. School of Eng.

Significant progress has been made in frequency modulation atomic force microscopy (FM-AFM) in liquids over the past few years, which allows us to directly investigate solid-liquid interfaces as well as "in vivo" molecular-scale biological processes. One of the major difficulties in FM-AFM imaging in low Q-factor environments was a large increase in the phase noise of the self-oscillation loop for the cantilever. Recently we successfully reduced the phase noise by decreasing the coherence of the laser light used in the cantilever deflection sensor.

In this presentation subnanometer-resolution imaging of crystalline surfaces as well as biomolecules in liquids using the improved FM-AFM is described. FM-AFM imaging of a muscovite mica surface in pure water revealed the honeycomb structure of SiO₄ tetrahedrons with a period of 0.52 nm. Recent atomic-scale study of calcite surfaces in aqueous solution is also presented. Furthermore, we also imaged a purple membrane consisting of hexagonally packed bacteriorhodopsin protein molecules in a phosphate buffer solution by FM-AFM. An array of protein trimers was clearly imaged. Furthermore, plasmid DNAs (pUC18, 2686 bp) adsorbed onto a mica surface were imaged by FM-AFM in a buffer solution containing 50 mM NiCl₂. We succeeded in visualizing individual phosphate groups composing the DNA backbone chains.

In addition, we recently found that frequency shift vs distance curve measured in water by FM-AFM reflects a local hydration structure. The oscillation structures with a period of about 0.2 - 0.3 nm, which is similar to the size of the water molecule, reproducibly appeared in the frequency shift curves. This new method for the investigations of local hydration structures was combined with the force mapping method, where forces (frequency shifts) are three-dimensionally mapped by measuring the force (frequency shift) curves over the sample surface. The frequency shift signal was recorded while the AFM tip was scanned in the vertical (z) and horizontal (x) directions on a mica substrate in water. As shown in Fig.1, the results reveal that there are three/four water layer structures with slightly different spacings on the surface and that the closest layer to the surface has an atomic-scale horizontal structure reflecting the surface crystal structure of muscovite mica. The obtained hydration structure was compared with water density distributions calculated using the 3D reference interaction site model (3D-RISM) theory.

Figure 1. Two-dimensional (x and z directions) frequency shift mapping (gray contrast) in a KCl aqueous solution on a mica crystal surface.



Keywords: solid-liquid interface, hydration structure, atomic force microscopy, FM-AFM, surface atomic structure

MIS020-04

Room:301A

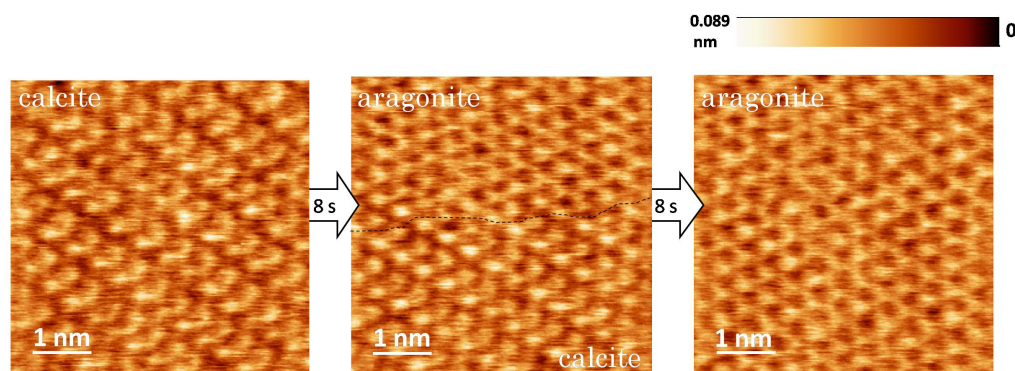
Time:May 24 15:30-15:45

Atomic in situ investigation of aragonite formation by FM-AFM

Yuki Araki^{1*}, Katsuo Tsukamoto¹, Mihoko Maruyama², Tomoyuki Miyashita³, Noriaki Oyabu⁴, Kei Kobayashi⁴, Hirohumi Yamada⁴

¹Sci., Tohoku Univ., ²Eng., Osaka Univ., ³Biology Sci. and Tech., Kinki Univ., ⁴Eng., Kyoto Univ.

The crystallization by the interactions between organic materials and inorganic minerals is called "biomineralization". Although aragonite is metastable at normal temperature and pressure, some bivalve shells contain prismatic calcite and nacreous aragonite simultaneously by using special proteins (Falini et al., 1996, Belcher et al., 1996). We have done in situ observation of aragonite formation in atomic resolution on calcite seed crystal in the solution containing the synthetic polypeptide, which imitates the sequence of amino acids in the special proteins (Takagi and Miyashita, 2010). As a result, it was confirmed that calcite transformed to aragonite in the surface layer of calcite seed crystal, and the synthetic polypeptide adsorbed along calcium sequence of calcite [010]. Our results strongly suggest there is the new model of aragonite formation under normal condition.



Keywords: biomineralization, the synthetic polypeptide, Frequency Modulation AFM

Japan Geoscience Union Meeting 2011

(May 22-27 2011 at Makuhari, Chiba, Japan)

©2011. Japan Geoscience Union. All Rights Reserved.



MIS020-05

Room:301A

Time:May 24 15:45-16:00

Crystal growth of Scorodite crystals by UV light irradiation

Ryuichi Komatsu^{1*}, Hideyuki Okamura¹, Masakazu Nagai¹, Hironori Itoh¹

¹Graduate School of Seg.&Sci., Yamaguchi

Considerable amounts of arsenic by-products in metallurgical processes have usually been stored because of its little demand. Stored arsenic is poisonous. Therefore, various stable fixation processes of arsenic have been investigated and in particular, scorodite ($\text{FeAsO}_4 \cdot 2\text{H}_2\text{O}$) synthesis has been paid much attention because of its low solubility. Most important issue in scorodite synthesis is to grow large-sized scorodite particles to keep low solubility.

Fujita et al. reported that the largest scorodite particle is 15 micron m in diameter. In this paper, in-situ observation to reveal growth behavior of scorodite crystals has been performed and growth conditions have been investigated. A novel scorodite synthesis method has been developed. The maximum size of grown scorodite crystal by this method is about 60 micron m.

Keywords: UV light, Scorodite, Crystal growth

MIS020-06

Room:301A

Time:May 24 16:00-16:15

the Mechanism of Emergence of Chirality in NaClO_3 Crystals from a Solution

Hiromasa Niinomi^{1*}, Takahiro Kuribayashi¹, Hitoshi Miura¹, Katsuo Tsukamoto¹

¹Graduate School of Science, Tohoku Univ.

Chiral symmetry breaking in sodium chlorate (NaClO_3) crystallization from a solution was reported by Kondepudi et al.(1990)[1]. The chiral NaClO_3 crystal is cubic, and its space group is $P2_13$. When NaClO_3 crystals crystallized from a static solution by evaporation, equal numbers of L-crystals and D-crystals appeared. In contrast, from a stirred solution, almost only one type of crystals appeared. This significant bias of chirality is termed as chiral symmetry breaking. Although there are some theories about the process that causes the chiral symmetry breaking, the real process has not been elucidated yet. To obtain the direct evidence of chirality symmetry breaking, we carried out in-situ observation of crystallization process from a NaClO_3 solution by polarization microscope. As a result of the observation, it was found that non-cubic metastable crystals appeared from the solution at first, and then, the crystals transformed to cubic crystals by a solid-solid phase transition or a solution-mediated phase transition [2].

If the metastable crystal does not have chirality, it can be said that chirality of the cubic crystal emerges when the phase transition occurs. However, since the structural analysis of the metastable crystal has not been carried out, it is not clear whether the metastable crystal has chirality or not. It is important to clarify the crystal structure of the metastable crystal for a new understanding of chiral symmetry breaking in the NaClO_3 solution.

The object of this study is to clarify the mechanism of chiral symmetry breaking in a NaClO_3 solution by measuring the crystal structure of the metastable phase by means of single-crystal X-ray diffraction experiment.

The metastable crystal was prepared by drop evaporation method as follows. A drop (6 microliter) of a NaClO_3 solution saturated at room temperature(293K) was put onto a cover glass. The metastable phase crystallized out in the drop as the solution evaporated. After the crystal grew up to 200 micrometer in size, we replaced the drop with glycerin. At the end, the crystal and the drop of glycerin were frozen by liquid nitrogen. The frozen drop is the specimen for the X-ray diffraction analysis. We used Imaging plate type single-crystal X-ray diffractometer (R-AXIS IV++, Rigaku). To keep specimen frozen during the analysis, temperature around the specimen was kept at -266 ± 1 (K) by Cryostream (Oxford). Analytical method is the oscillation method.

As a result, we determined the lattice constant, crystal system and space group of the metastable phase as follows; $a=8.42$ (Å), $b=5.26$ (Å), $c=6.70$ (Å), β angle= 109.71° , monoclinic, and $P2_1/a$, respectively. These values are very similar to that of NaClO_3 (I), which is high temperature phase of NaClO_3 crystal in melt growth ($a=8.78$ (Å), $b=5.17$ (Å), $c=6.83$ (Å), β angle= 110° , monoclinic, and $P2_1/a$) [3]. Therefore, it is highly possible that the metastable phase is the same as the NaClO_3 (I) phase. In addition, a crystal having a space group of $P2_1/a$ does not have chirality, that is to say, the metastable phase that we obtained from the solution does not have chirality. From these results, we concluded that chirality of the cubic NaClO_3 crystal emerges when the phase transition occurs.

In this study, we revealed that the metastable phase of NaClO_3 crystal in solution growth does not have chirality. It also becomes clear that chirality of a cubic crystal emerges when the solid-solid phase transition occurs.

References

- [1] D. K. Kondepudi, R. J. Kaufman and N. Singh, (1990). Science. Vol.250, pp.975-976
- [2]H. Niinomi, K. Tsukamoto, M. Uwaha, H. Miura, Japan Geoscience Union Meeting 2010, MIS012-06
- [3]P. Meyer and M. Gasperin, (1973). Bull. Soc. Fr. Mineral. Cristallogi. Vol.96, pp18-20

Keywords: Chiral Symmetry Breaking, Sodium Chlorate, in-situ observation, X-ray structural analysis, metastable phase, phase transition

MIS020-07

Room:301A

Time:May 24 16:30-17:00

Galaxy-like magnetic domain structures in ferromagnetic nanoparticle arrays observed by electron holography

Kazuo Yamamoto^{1*}

¹Japan Fine Ceramics Center

When ferromagnetic nanoparticles are packed as a face-centered-cubic (fcc) lattice, dipolar ferromagnetic state appears in the lattice film. Magnetic dipoles in each nanoparticle are aligned in one direction with dipole-dipole interaction. This ground state was theoretically predicted by Luttinger and Tisza in 1946 [1]. Magnetic force microscopy (MFM) detected collectively magnetized regions in 12 nm Co nanoparticle assemblies [2]. However, the magnetic domain structures have been obscure because MFM is not sensitive enough to image the in-plane component in the arrays. Electron holography, one of the techniques using a transmission electron microscope (TEM), can detect and image the in-plane component of magnetic flux at higher spatial resolution. Here, we report our use of electron holography to observe the existence of dipolar ferromagnetic domain structures and their behavior.

We prepared 8 nm epsilon-Co nanoparticles by thermally decomposing cobalt carbonyl precursor in high boiling-point solvent. Each nanoparticle was coated with organic surfactants. We dispersed the particles on immiscible liquid and compressed them to obtain close-packed monolayers. We then transferred them to carbon-coated TEM grids [3]. Before loading the sample into the TEM, the film was scratched with a sharp tungsten needle to obtain a vacuum area for electron holography.

Figure 1 shows the TEM image of the particle arrays with partial disordering. The average edge-to-edge separation between particles is 4.2 nm, so exchange effects are minimal. We used Philips CM200 field emission TEM under Lorentz microscopy mode; the standard objective lens was turned off and a Lorentz mini-lens beneath the objective lens was used to focus the sample. To observe virgin domain structures of dipolar ferromagnetism, we cooled the sample to 108 K with a liquid nitrogen cold stage in a field free environment (Zero Field Cooling).

Figure 2(a) shows a 7.5 micron wide region of the array. We took a series of holograms and reference holograms at the same positions, and obtained the magnetic flux distribution shown in Figure 2(b). We observed partially galaxy-like structures in micron scale that were separated by transverse domain walls. A previous simulation predicted vortex structures due to magnetostatic interactions [4]. Our result was similar to the simulation pattern at the sample edges.

Next, we applied a magnetic field to the sample in the TEM. The sample was tilted and the objective lens was turned on. After turning off the lens, the sample was tilted back and imaged in remanence. The center of the galaxy-like structure was shifted to the left, as shown in Figure 2(c). Shifting of a transverse wall by a magnetic field has also been observed in ordinary ferromagnetic permalloy rings [5]. A similar response occurred in our sample without exchange coupling.

We demonstrated the existence of dipolar ferromagnetic domain structures formed in the magnetic nanoparticle arrays, and observed the patterns of the domain structures and their response to the applied field. This observation should clarify the characterization of dipolar ferromagnetism in nanoparticle arrays.

Acknowledgements

We are grateful to Prof. S. A. Majetich and Dr. M. Sachan in Carnegie Mellon University for preparing the sample and valuable discussion. We thank to Prof. S. Yamamuro, Dr. T. Hirayama, Prof. M. R. McCartney and Prof. D. J. Smith for important comments in holography images. We gratefully acknowledge the use of facilities within the John M. Cowley Center for High Resolution Electron Microscopy at Arizona State University.

References

- [1] J. M. Luttinger, L. Tisza, Phys. Rev. 70, 954-964 (1946).
- [2] V. F. Puntes et al., Nature Mater. 3, 263-268 (2004).
- [3] M. Sachan et al., J. Appl. Phys. 99, 08C302 (2006).

[4] A. J. Bennett, J. M. Xu, Appl. Phys. Lett. 82, 2503-2505 (2003).
 [5] T. Uhlig, J. Zweck, Phys. Rev. Lett. 93, 047203 (2004).

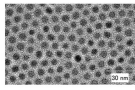


Fig. 1. TEM image of 8 nm epsilon-Co nanoparticle array.

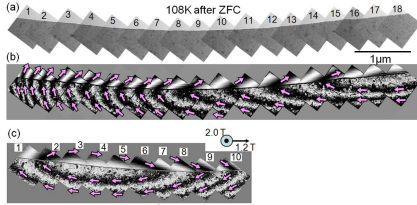


Fig. 2. Dipolar ferromagnetic domain structure after zero field cooling. (a) A series of 18 TEM images taken along the edge of the array film. (b) Magnetic flux distribution around the edge. (c) Magnetic flux distribution after applying magnetic field in the TEM.

Keywords: electron holography

MIS020-08

Room:301A

Time:May 24 17:00-17:15

Production of Co nanocrystals from a C-Co mixture amorphous film and Oriented Crystallization of Carbon

Hitoshi Suzuki⁵, Yoshiro Miura^{1*}

¹Yoshiro Miura, ²Aakihito Kumamoto, ³Chihiro Kaito, ⁴Jun Onagawa, ⁵Hitoshi Suzuki

Pt nanoparticles were used as a catalyst of a fuel cell. The catalyst consists of Pt nanoparticles put on onion-like carbon particles as a substrate. The Pt catalyst degraded by a growth of Pt nanoparticles and an alteration of the onion-like carbon structure. Because of a high price and poor resources, a low Pt catalyst by an additive of another metal or a new catalyst without Pt were studied. However, an effect of the additive materials on the degradation of the catalyst was not studied. In order to confirm the effect of degradation, we tried to grow several metal particles in an amorphous carbon film as a model experiment. In the case of Co nanocrystals, the structure of carbon changed with Co nanoparticles growth.

The C-Co mixture amorphous film was produced by co-evaporation of carbon and Co in vacuum. The film was heated in TEM from RT to 800°C by in-situ observation. TEM images and ED patterns of the film was taken every 200°C steps.

The co-evaporation film had uniform contrast and amorphous structure. On heating 400°C, black dots were deposited on the film and grew on rising their temperature. On heating 600°C, fcc-Co nanocrystals grew on the film like the black dots and diamond-like ring was appeared in the ED pattern. Above 600°C, the black dots began moving on the film and some contrasts like a wheel truck appeared on the film after the black dots moving. The truck contrasts may produce by absorption of carbon atoms into the fcc-Co nanocrystal and diffused onto the surface again. When the absorbed carbon atoms diffused onto the surface, fcc-Co nanocrystals moved and microcrystallites of carbon with the truck like contrasts deposited on the film. In ED pattern, weak ring of (002) of the graphite appeared on heating 800°C.

To examine the diamond-like ring, ED pattern in a folded part of the film was observed after the heat treatment. The ring of graphite (002) perpendicular to the folded line of the film became strong in the ED pattern. The folded line of the film became white in a dark image from the strong ring. And graphite (002) lines were observed by HREM image of the folded part. Therefore, the origin of the diamond-like ring appeared in the ED pattern on heating 600°C was microcrystallites of oriented graphite of c-axis. The graphite may be crystallized on an interface of the fcc-Co particles and the amorphous film by diffusion of carbon atoms on heating 600°C.

Keywords: Nanoparticles, Crystallization, Co, Carbon, TEM, amorphous film

MIS020-09

Room:301A

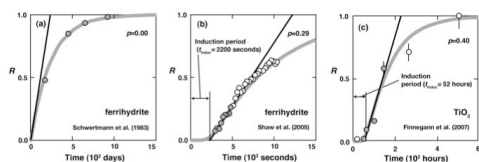
Time:May 24 17:15-17:30

Kinetic theory of crystallization of nanoparticles

Katsuhiro Tsukimura^{1*}, Masaya Suzuki¹, Yohey Suzuki¹, Takashi Murakami²

¹AIST, ²The University of Tokyo

We here describe a kinetic theory of the crystallization of nanoparticles, where nanoparticles are dissolving and crystals are forming in solution. The theory assumes that a crystal nucleates only on a nanoparticle, the crystal stops growing at a certain size, and the concentration of metal ion in solution is close to the solubility of the nanoparticles. On the basis of these assumptions, we have derived integral equations for $R(t)$ (crystal ratio as a function of time). We have solved the integral equations with a successive approximation method. When time t is less than t_{inflec} ($=r_{max}/G$, r_{max} : maximum radius of crystal, G : growth rate of crystal), $R(t)$ is close to fourth power of time; when t is larger than t_{inflec} , $R(t)$ is close to an exponential-type function. The kinetic theory has been applied successfully to the transformation of ferrihydrite nanoparticles to goethite or hematite crystals, and the crystallization of TiO_2 (Fig. 1). The theory shows that the nucleation rate of crystal essentially determines the crystallization rate, and that induction period is observed when the growth of crystal is slow. Some non-thermodynamic parameters such as the turbulence of solution and the size of system can also affect the crystallization rate. For example, the stirring of solution prevents crystals to deposit and makes the crystals grow larger, which in turn makes the crystallization rate high.



Keywords: kinetic theory, nanoparticle, nucleation, growth, ferrihydrite, titania

MIS020-10

Room:301A

Time:May 24 17:30-17:45

High-speed in-situ observation of a pulse homogeneous nucleation process in vapor phase

Yuki Kimura^{1*}, Hitoshi Miura¹, Katsuo Tsukamoto¹

¹Tohoku University

The gas evaporation method has a history of almost half century. Study of the products has been performed energetically mainly using a transmission electron microscope and elucidated that nanoparticles have different physical properties from that of the bulk material, have a crystal habit reflected their crystal structure as well as bulk crystals, and so forth. On the other hand, there is almost no report concerning a nucleation in a smoke in view of crystal growth. Recently, we firstly achieved an in-situ observation of a nucleation process in a smoke using a Mach-Zehnder type interferometer and clearly showed that smoke particles condense only in very high-supersaturation environment homogeneously. In case of preliminary experiment using tungsten trioxide, it condenses with a degree of supersaturation as high as $\sim 10^6$. In this process, since evaporant is continuously supplied into surrounding of an evaporation source, flow of a smoke (i.e., nucleation and growth of nanoparticles) has been simply considered as a consecutive process. However, the nucleation and growth of smoke particles should be a rapid process (\sim ms) due to high supersaturation. In such case, it is possible that the concentration of the evaporated vapor around the evaporation source is frequently changing. No one ever observed the detail of smoke formation process so far. There is only a report, which includes a serial photographs of a smoke and flow velocities were estimated as a function of gas pressure (Yatsuya et al. 1984). In this report, we tried to see a motion of a smoke using a high-speed camera (Keyence VW-9000) with a high-speed color camera (Keyence VW-600C) combined with a zoom lens of VH-Z20W to know the nucleation process of smoke particles.

A small vacuum chamber was newly constructed based on a new concept to do smoke experiments flexibly. The work chamber used was a stainless-steel cylinder 76 mm in diameter and 16 cm in length with two view ports of ICF70 for optical observation, a ports of ICF34 for temperature measurements using pyrometer, two electrodes and two tubes with quarter inch diameter for introduction of a thermocouple and a vacuum and gas system. Tungsten wire (99.95% in purity) with 0.3 mm in diameter and 70.0 mm in length was prepared as an evaporation source between the electrodes. After evacuating the chamber down to $\sim 10^{-2}$ Pa, Ar gas (99.9999% in purity) of 3.6×10^4 Pa and oxygen (99.999% in purity) gas of 4.0×10^3 were introduced into the chamber. The pressure was monitored by a capacitance manometer (ULVAC CCMT-1000D) and a pirani/cold cathode combination gauge (Pfeiffer PKR 251).

When a tungsten wire is electrically heated in the gas atmosphere, a tungsten wire reacts with oxygen and tungsten oxide smoke particles are produced. The smoke follows a convection current from bottom to top generated by a hot source. The high-speed camera was set in a direction of certainly parallel to the evaporation source and observed the smoke with a rate of 4000 frames per sec. As a result, we found a fluctuation with a constant frequency with ~ 11 ms of concentration of a smoke. We will discuss the reason why the concentration of a smoke fluctuates at the presentation. It can be assumed that decrease of a supersaturation is the reason. But, why? There is some possibilities; temperature increase due to latent heat by condensation, depletion of oxygen around the evaporation source and decrease of the concentration due to nucleation, which eats ambient tungsten oxide molecules immediately. We intend further experiment using gold, which will elucidate the reason more clearly.

Keywords: nucleation, dust, nanoparticle, in-situ observation

MIS020-11

Room:301A

Time:May 24 17:45-18:00

Allende meteoritic nanodiamonds and their possible shock wave formation

Arnold Gucsik^{1*}

¹Tohoku University, Dept Earth Sci

Two main theories exist for the formation process of the meteoritic nanodiamonds (e.g., Daulton et al. 1996-and references therein): (1) Chemical vapor deposition (CVD), and (2) shock origin. TEM investigations, in particular, seem to suggest that formation by a CVD process is most likely.

According to supernova shock wave experiment of Hansen et al. (2007) the first step is the transition of the secondary shock wave through interstellar media nearby the supernova explosion resulting the grain-grain collisions. The initial shock wave occurs rapidly, which can give the physical conditions such as high pressure and high temperature adequately for the formation of diamond creating the second stage or the crystallization stage. A disadvantage of this process, however, is that, pressures obtained during such collisions are often so high that shattering, sputtering and vaporization become dominant over phase transformation (Tielens et al. 1987, Jones et al. 1994, 1996), which limits the effectivity of diamond formation.

In conclusion, these results from the previous literature alone are not conclusive, especially since it is currently difficult to distinguish between the effects of shock transformation and small grain size. They leave open, however, the possibility that a significant fraction of the nanodiamonds in primitive meteorites were formed by shock transformation from graphite/amorphous carbon in the interstellar medium. As noted above, this possibility has been immediately recognized after their discovery (Tielens et al. 1987), but more recent works have mostly concluded that a CVD-like process is more likely (e.g., daulton et al. 1996, Le Guillou et al. 2006, 2007). However, CVD theory does not explain details on the 2.6 nm as an average size of the meteoritic nanodiamonds, which may be related to the H-or N-related self-terminating crystal growth process (Sun et al. 2004) in the shock-wave front. On the other hand, the surface chemistry of the nanodiamonds shows a poor thermal stability between 850-1350 oC (Lu et al. 2007) indicating the low-temperature crytallization process of the single diamond grains. These factors may also support the shock wave origin of the meteoritic nanodiamonds.

Other processes that are possible in principle (see also Anders and Zinner 1998), but have received less attention, are photolysis of hydrocarbons (Buerki and Leutwyler 1991), annealing by UV photons (Nuth and Allen 1992) and transformation by energetic particle irradiation (e.g., Ozima et al. 1997).

Keywords: Allende, supernova, nanodiamonds, shock wave, interstellar media, meteorite

MIS020-12

Room:301A

Time:May 24 18:00-18:15

Growth Rate Measurement of Lysozyme Crystal using Interferometry for Space Experiment

Tomoya Yamazaki^{1*}, Hitoshi Miura¹, Yuki Kimura¹, Izumi Yoshizaki², Takao Maki³, Katsuo Tsukamoto¹

¹Graduate School of Science, Tohoku Unive, ²Japan Aerospace Exploration Agency, ³Olympus Corporation

The growth rate of a lysozyme crystal in the solution under microgravity condition was measured at the Foton-M3 mission [1] and at the parabolic flight experiment [2]. In both cases, the growth rate under microgravity condition was larger than that under terrestrial condition. It was considered that the lack of buoyancy convection under the microgravity modifies the distribution of impurity molecules nearby the crystal-solution interface. However, the reason why the growth rate increased under microgravity was still not clear because the experimental data of the growth rate under microgravity was limited. In order to answer this question, we are planning to measure the growth rate of the lysozyme crystal under microgravity condition at the International Space Station by in-situ observation.

We employ Michelson interferometer for the growth rate measurement at the Space experiment. The Michelson interferometer is the strong instrument for the surface observation and the growth rate measurement because nano-order difference in height on the crystal surface can be measured by the interference fringes. However, the problem for the growth rate measurement using the interferometer is the external disturbance like mechanical vibration and temperature changes, which makes difficult the measurement by moving the fringes. To avoid such disturbances, Tsukamoto et al. used the cell glass surface, on which a sample crystal settled, as a reference to cancel the disturbance from the growth rate measurement [3]. Sato et al. used gold particles settled on the sample crystal surface as the reference [4]. These techniques are very powerful to measure the growth rate precisely, however, they are not applicable for the Space experiment because of the following reasons. First, the reflected light from the lysozyme crystal surface is too weak comparing with that from the glass surface to observe clearly. Second, for the space experiment, gold particles cannot be used because they may not settle on the crystal surface but float in the solution under the microgravity condition. To solve these problems, we use a glass plate is used as the reference to evaluate the external disturbance in the measurement of the growth rate by using Michelson interferometer.

We set up the Michelson interferometer and carried out the growth rate measurement of lysozyme crystal on the ground as a pre-experiment. We put the glass plate at the side of the lysozyme crystal and observed surfaces of the crystal and the glass plate simultaneously. The movement of the fringes on the glass plate is only due to the external disturbance, therefore, it is used to cancel the disturbance from the fringe movement on the crystal surface. We obtained the growth rate of the lysozyme crystal and compared the measured growth rate with the previous measurement [5]. We succeeded to measure the growth rate of an order of 0.01 nm/s appropriately by the Michelson interferometer.

References

- [1] Tsukamoto et al. (2008). *J. Jpn.Soc.Microgravity Appl.*25, 4, 730.
- [2] Yamazaki (2010). Master thesis, Tohoku Univ.
- [3] Tsukamoto et al. (1998). *J. Jpn.Soc.Microgravity Appl.*15, 2-9.
- [4] Satoh et al.(2007). *Am. Mineral.* 92, 503-509.
- [5] Dold et al. (2006). *J. Cryst. Growth* 293, 102-109.

Keywords: lysozyme, crystal growth rate, interferometry, microgravity

MIS020-13

Room:301A

Time:May 24 18:15-18:30

Development of 3-D interferometer for crystal growth

Kenta Murayama^{1*}, Katsuo Tsukamoto¹

¹Graduate School of Science, Tohoku Unive

To understand the mechanism of crystal growth in solution, it is very important to know the concentration field around the growing crystal, especially, around the crystal-solution interface. Growth mechanism changes as the supersaturation increases. The solute concentration near the crystal-liquid interface, however, is smaller than that of the bulk solution because the crystal grows by incorporating solute in the solution. Local concentration distribution in the crystal interface can cause instability of the form on the crystal surface, it is important to determine the concrete concentration distribution in the crystal interface to discuss the mechanism of the crystal growth. Therefore, to discuss the relation between the crystal growth mechanism and growth rate of the crystal, it is necessary to measure the concentration around the crystal-liquid interface, not of the bulk.

There were many previous researches of measurement of the concentration field, but many of them were two-dimensional (2-D) observations, namely, only from one direction. However, the information obtained by the 2-D observations is integrated along the direction of the observation, so the local information, e.g., concentration around the crystal-liquid interface, is not obtained.

To solve the problem on the 2-D observation, a method of computer tomography (CT) has been adopted by some authors. By using the CT method, one can reconstruct the information of the three-dimensional concentration field around the growing crystal based on 2-D observations obtained from several directions (3-D observation). Previous works of 3-D observations revealed the three-dimensional structure of solute convection around the growing crystal. However, there is quite a few observations of the concentration field around the crystal-solution interface.

In the present study, we carry out 3-D observation to measure the three-dimensional concentration field very close to the crystal-liquid interface growing in solution quantitatively. We newly develop two types of optics; microscopic Mach-Zehnder interferometer.

For quantitative 3-D measurement of concentration field, we developed 3-D microscopic Mach-Zehnder interferometer. 3-D observations by using our newly developed microscopic Mach-Zehnder interferometer can provide us the detailed information of concentration field around a growing crystal with high magnification and high sensitivity.

For the application of the 3-D observation by using our Mach-Zehnder interferometer, we measured the concentration field around protein crystal growing in solution. The growth rate of the protein crystal is quite low, so the decrease of concentration in solution should be much smaller. The interference fringes obtained are straight, but curved slightly only in a very narrow area close to crystal surface. In spite of the very small movements of the interference fringes, we successfully reconstructed the 3-D concentration field around the growing protein crystal. From the reconstructed image, we identified two low concentration regions on the vicinity of the crystal surface. These positions corresponded to the positions of spiral growth centers, which were observed by the confocal laser scanning microscope just after the growth experiment. The 3-D reconstruction of the concentration field around a protein crystal growing in solution was performed for the first time in this work.

This is the first time to confirm the correlation between the position of spiral growth center on the growing crystal surface and the low concentration region obtained by the 3-D reconstruction. The 3-D observation system we developed in this study is a powerful tool to obtain the experimental data concerning the interaction between the concentration field and the layer-by-layer growth mechanism on faceted crystal surface. It is expected that we can deepen the understanding of the layer-by-layer growth theory based on the result of the quantitative 3-D observation.

MIS020-P01

Room:Convention Hall

Time:May 24 10:30-13:00

Formation mechanism of domain structure and defect of goethite surface

Takuya Echigo^{1*}, Tamao Hatta¹, Seiko Nemoto¹, Shigeru Takizawa²

¹JIRCAS, ²University of Tsukuba

Goethite (alpha-FeOOH) is one of the most common iron (oxyhydr)oxide minerals in surface environment of Earth and has huge specific surface area due to the small particle size. The surface of goethite plays an important role in many chemical reactions, e.g., adsorption, dissolution and precipitation, and thus their mechanism and kinetics are studied in detail using synthetic goethite. However goethite occurring in natural environment shows wide range of crystallinity (Kuhnel et al., 1975) and it is known that many properties, e.g. *a*-dimension of the unit cell and OH bending mode, are affected by the crystallinity (Schwertmann et al., 1985). Goethite with low crystallinity shows multidomain structure and weak hydrogen bonds owing to the -OH defects in the crystal structure and those characteristics accelerate the dissolution and adsorption rates (Strauss et al., 1997). In this study, we investigate the surface morphology and the ratio of surface hydroxyl group to oxygen, $[-OH]/([-O] + [-OH])$, of goethite with varying crystallinity and discuss the formation mechanism of multidomain structure and OH defects.

Goethite in this study was synthesized using ferric nitrate ($Fe(NO_3)_3 \cdot 9H_2O$) and potassium hydroxide (KOH) as starting materials, according to Schwertmann et al. (1985). The dark brown precipitate, which is amorphous ferric oxide called ferrihydrite, was aged for 70 days at 4 °C (G-04), 30 days at 30 °C (G-30), 10 days at 50 °C (G-50) and 3 days at 70 °C (G-70). All products were washed with pure water, dried in nitrogen atmosphere and identified as goethite by powder XRD analysis. The morphology of these goethite were observed using AFM and specific surface area were measured with 11-points BET method. X-ray photoelectron spectroscopy (XPS) was employed to analyze the ratio of surface hydroxyl groups to surface oxygen.

AFM observations revealed that all goethites have acicular morphology, however, goethite aged at high temperature has larger particle size (> 1000 nm), higher aspect ratio and monodomain structure. On the other hand, goethite aged at low temperature has smaller particle size (< 200 nm), lower aspect ratio and multidomain structure. This observation well agrees with TEM observation by Schwertmann et al. (1985). XPS analysis revealed that the ratio of surface hydroxyl group to oxygen, $[-OH]/([-O] + [-OH])$, was higher for the goethite aged at higher temperature.

Transformation of ferrihydrite into goethite proceeds in three stages (Cornell et al., 1989; Yuwono et al.): (1) crystallization of goethite nanoparticles from ferrihydrite nanoparticles, (2) oriented attachment of goethite nanocrystals and (3) development of crystal morphology by aging. In aging at high temperature, ferrihydrite nanoparticles crystallize rapidly and completely, and thus oriented attachment occurs without misalignments. As a result, goethite aged at high temperature has monodomain structure and high aspect ratio. On the other hand, in lower temperature, ferrihydrite crystallizes into goethite nanoparticles slowly and incompletely, hence aggregation of the goethite nanoparticles has many misalignments. The multidomain structure, OH defects and low aspect ratio of goethite aged at low temperature arise from the misalignments within the aggregate of nanoparticles as a precursor of aged goethite.

Keywords: crystallinity, crystal morphology, particle size, AFM, XPS

MIS020-P02

Room:Convention Hall

Time:May 24 10:30-13:00

DNA nano-structure formation and the interpretation based on crystal growth theory

Yuya Ueno¹, Hitoshi Miura^{1*}, Shogo Hamada², Satoshi Murata³, Katsuo Tsukamoto¹

¹Tohoku University, ²Tokyo Institute of Technology, ³Tohoku University

The DNA molecule is now attracting attention as a new self-assemble material. The reason why DNA is used for self-assembly is that DNA molecule has calculation capability. Many nanostructures have been produced using DNA, for example, DNA tile (Winfrey and Seeman, 1998). DNA tile is a complex molecule, which is composed of some single strand DNA (ssDNA). Each tile has some sticky ends (a part of some exposed bases). The complementary sticky end spontaneously makes hydrogen bond and grow to large ordered structure (DNA tile crystal) as the solution cools down. This process is termed as self-assembly, in other words, crystallization. Although DNA tile has potential as computer, there are some problems. The most important matter is presence of error (misfit crystallization). In order to reduce this error, many types of DNA tiles have been designed. However, it is difficult to completely prevent the assemble error. For synthesis of DNA tile crystal without the assemble error, we carried out experimental study of DNA tile formation and interpreted the result based on crystal growth theory.

First, we chose T-motif as DNA tile, which is able to grow on the electrically-charged Mica surface like two dimensional crystal, and measured its growth rate using DNA origami as a seed crystal with atomic force microscopy. The growth rate of T-motif crystal on Mica substrate was about 4.30 [monomers/minute].

In the second experiment, we observed T-motif crystals synthesized on the Mica surface for various conditions (temperature and concentration). We found that the nucleation temperature of the T-motif crystal was about 41.5 [deg. C.], which did not depend on the concentration significantly in a range of 2~10 [nM]. From this result, we assumed that the T-motif crystal growth can be considered to be melt growth. In order to understand the growth mechanism, we calculated the step free energy β [J/m] and melting point T_m [deg. C.] under the assumption that the number density of crystals on the Mica surface is proportional to the two-dimensional nucleation rate. When the melting point is assumed to be 50 [deg. C.], the calculated step free energy was about 4.21×10^{-13} [J/m]. The calculated step free energy of T-motif crystal is similar to that of Lysozyme crystal (8.9×10^{-13} [J/m]).

We also observed the morphological change of T-motif crystals depending on the growth condition. In the highest supersaturation condition in this study (T-motif concentration is 10 [nM] and temperature is 38 [deg. C.]), the morphology of the T-motif crystal was similar to dendrite crystal. In other cases, the morphology was found to be polygonal shape. The reason why the T-motif crystal becomes dendritic in the highest supersaturation condition is considered to relate to the thermal stability of the sticky end binding. In low supersaturation, many T-motif units bind only at a site with two sticky ends. In contrast, in the highest supersaturation, the T-motif unit can bind to anywhere. We calculated the difference of Gibbs free energy in two conditions; one match bond of sticky end or two matches. We found that when the driving force exceeded the critical point, the T-motif crystal has possibility to be formed as dendrite. Using the critical driving force, we calculated the temperature at which the T-motif dendrite crystal was formed. In this calculation, the temperature of dendrite formation is 41.8 [deg. C.] when the melting point is assumed to be 50 [deg. C.]. On the other hand, experimental result shows that T-motif dendrite form in 38 [deg. C.]. The inconsistency between the theory and the experiments should be resolved in the future, however, our study is an important first step to describe the growth mechanism of the T-motif crystal based on the theory of crystal growth from melt phase.

Keywords: DNA tile, Crystal growth

MIS020-P03

Room:Convention Hall

Time:May 24 10:30-13:00

The morphological relationship of octacalcium phosphate and its precursor: the role of intermediate phase

Yuki Sugiura^{1*}, Kazuo Onuma², Yuki Kimura¹, Hitoshi Miura¹, Katsuo Tsukamoto¹

¹Department of Science, Tohoku University, ²Human life technology, AIST

Octacalcium phosphate (OCP) is the precursor of hydroxyapatite (HAP) which is main component of human tissue. HAP crystals which form through OCP are pseudomorph of OCP. Thus, the investigation of OCP morphological decision is connected with the later phase, HAP morphological decision. In around neutral pH solution, amorphous calcium phosphate (ACP) is precipitated as an initial solid phase at supersaturated calcium phosphate solution. Wherein, we investigated the formation process of characteristic morphology of OCP from ACP in solution.

We prepared 1 mol/L CaCl₂ and 0.5 mol/L KH₂PO₄ solutions which were also buffered by tris amino methane, and 0.15 mol/L tris amino methane-HCl buffer solution. These three solutions were gently blended without stirring to observe the morphological connection between initial phase and later phase through the materials evolution of calcium phosphates precipitations in solution by field emission scanning electron microscopy (FE-SEM), transmission electron microscopy (TEM) and X-ray diffraction (XRD). (The total concentration is Ca = 0.075 mol/L, PO₄ = 0.045 mol/L, tris amino methane = 0.015 mol/L, 32C, initial pH = 7.7) Immediately after blending, white indeterminate precipitates were emerged and formed gel-like structure which was maintained for 40 minutes after blending. The solution pH was gradually decreasing around 4 until 40 minutes later. In FE-SEM and TEM observation, the gel-like structure was consisted of sphere-like ACP particles with 100 nm in diameter and ACP spherulites with 3-20 micro meter in diameter. In proceeding time, fiber-like beat-tri calcium phosphate crystals (TCP) were emerged in gel-like structure and ACP sphere particles were vanished. 3 minutes later, ACP spherulites transformed through TCP like phase. 6-12 minute later, the TCP like phase spherulites transformed spherulites which composed of both of single OCP crystal and TCP polycrystals. TEM dark field image showed OCP and TCP domains were mingled. Finally, the spherulites transformed into single OCP crystals with maintain their whole spheritic morphology until 40 minutes later. These observations suggested that OCP is pseudomorph of ACP. In below 7 pH solution, it suggested that through TCP like phase, morphology of OCP crystals was maintaining initial phase morphology, ACP.

Keywords: octacalcium phosphate, morphology, precursor, phase transition, pseudomorph

MIS020-P04

Room:Convention Hall

Time:May 24 10:30-13:00

In situ measurement of dissolution and growth velocities of $\text{Ca}(\text{OH})_2$ for CO_2 trapping

Yoshifumi Oshima^{1*}, Katsuo Tsukamoto¹, Hitoshi Miura¹, Yuki Kimura¹, Hisao Satoh²

¹Tohoku university, ²Naka Energy Research Laboratory, Mitsubi

In these latter days, CO_2 capture and storage (CCS) has attracted considerable attention as a greenhouse gas mitigation option against global warming problems. CCS is a technique to confine captured CO_2 to underground or sea for a long time. One of the trapping strategies is a mineralization of CO_2 , into calcite (CaCO_3) for instance. Since calcite is a stable polymorph of calcium carbonate on the earth, it is expected to trap CO_2 during a long term. To produce calcite, it has been investigated as a convincing reaction that calcium hydroxide ($\text{Ca}(\text{OH})_2$) crystal reacts with liquid containing CO_3^{2-} (Lacker et al., 1995). However we do not know how long the transformation takes for $\text{Ca}(\text{OH})_2$ crystal to calcite because there is no data of the growth and dissolution velocities of $\text{Ca}(\text{OH})_2$ crystal. The purpose of this study is to solve the growth and dissolution mechanism of $\text{Ca}(\text{OH})_2$ crystal by 'in situ measurement of these velocities of it'.

We adopted Phase-Shift Interferometer (PSI) for the measure of normal growth and dissolution rates of $\text{Ca}(\text{OH})_2$. Since PSI has extremely high spatial resolution as a few nm in vertical direction, it can detect ultra-slow normal velocity of crystal surface ($\sim 10^{-5}$ nm/s). We put a $\text{Ca}(\text{OH})_2$ crystal in a solution which is adjusted from -0.46 to 0.29 in supersaturation by mixing 4 liquids (0.25 M CaCl_2 , 0.50 M NaOH , 2.0 M NaCl solution and pure water which is completely degassed), and then measured the normal growth or dissolution rate of (001) face of the $\text{Ca}(\text{OH})_2$ crystal.

We expect that the growth pattern was multi-nucleation in supersaturation > 0 by normal growth rate depending on supersaturation because the normal growth rate rises sharply at a specific supersaturation. We obtained that step edge energy of two dimensional nucleus formed in multi-nucleation condition was 1.093×10^{-11} J/m by fitting into a theoretical formula for the first time. The value was smaller than that of calcite on (10-14) obtained from the previous work (Teng et al., 2000). The result is probably one of the reason that $\text{Ca}(\text{OH})_2$ crystal grows by multi-nucleation in the range of the low supersaturation.

In addition, on the basis of the result of $\text{Ca}(\text{OH})_2$ normal growth and dissolution rate, toward CO_2 mineral trapping we could predict how $\text{Ca}(\text{OH})_2$ crystal behaved during dissolution in $\text{Ca}(\text{OH})_2$ -calcite crystals system on the condition that calcium ion concentrations (supersaturation) were $[\text{Ca}^{2+}] > 10^{-2}$, $10^{-4.5} < [\text{Ca}^{2+}] < 10^{-2}$ and $[\text{Ca}^{2+}] < 10^{-4.5}$ M and that hydroxide and carbonate ion concentration and temperature were constant.

We inferred that the behavior of $\text{Ca}(\text{OH})_2$ -calcite crystals when they co-exist in the solution and found that calcite can grow sooner or later even if the solution is initially undersaturated for calcite. From these results, we concluded that the behavior of $\text{Ca}(\text{OH})_2$ crystal could be predicted in the various supersaturation systems understood the normal growth and dissolution rates as a function of supersaturation and CO_2 mineral trapping is enough to enable using $\text{Ca}(\text{OH})_2$ crystal, which is an important candidate material for CO_2 -storage in the future.

Keywords: calcium hydroxide, calcium carbonate, mineral trapping, multi-nucleation

Japan Geoscience Union Meeting 2011

(May 22-27 2011 at Makuhari, Chiba, Japan)

©2011. Japan Geoscience Union. All Rights Reserved.



MIS020-P05

Room:Convention Hall

Time:May 24 10:30-13:00

Carbon Sequestration

Katsuo Tsukamoto^{1*}

¹Gra. School of Science

Carbon sequestration will be discussed.

Keywords: Carbon Sequestration, Crystal Growth, Dissolution